Numerical Experiments on PF1000 Neutron Yield

S. H. Saw, D. Subedi, R. Khanal, R. Shrestha, S. Dugu & S. Lee

Journal of Fusion Energy

ISSN 0164-0313

J Fusion Energ
DOI 10.1007/s10894-014-9731-4

Springer

Your article is protected by copyright and all rights are held exclusively by Springer Science +Business Media New York. This e-offprint is for personal use only and shall not be self-archived in electronic repositories. If you wish to self-archive your article, please use the accepted manuscript version for posting on your own website. You may further deposit the accepted manuscript version in any repository, provided it is only made publicly available 12 months after official publication or later and provided acknowledgement is given to the original source of publication and a link is inserted to the published article on Springer's website. The link must be accompanied by the following text: "The final publication is available at link.springer.com".

Author's personal copy

J Fusion Energ
DOI 10.1007/s10894-014-9731-4

ORIGINAL RESEARCH

Numerical Experiments on PF1000 Neutron Yield

S. H. Saw · D. Subedi · R. Khanal · R. Shrestha · S. Dugu · S. Lee

© Springer Science+Business Media New York 2014

Abstract Numerical experiments are carried out, using the Lee model code to compute the neutron yield Y_n of PF1000 as a function of pressure. Computed results are compared with available published results of neutron yield. Relevant plasma focus properties such as peak discharge current I_{peak}, pinch current I_{pinch}, pinch ion density n_i and energy input into the pinch EINP are also discussed as functions of pressures so as to provide correlation of Y_n with relevant plasma focus properties over the operational range of pressures.

Keywords Plasma focus · Pinch · Neutron yield · Fusion

Introduction

The code [1] couples the electrical circuit with PF dynamics, thermodynamics and radiation. It is energy-, charge- and mass- consistent. It was described in 1983 [2] and used in the design and interpretation of experiments [3–5]. An improved 5-phase code [2] incorporating finite small disturbance speed [6], radiation and radiation-coupled dynamics was used [7–9], and was web-published [10] in 2000. Plasma self- absorption was included [10] in 2007. It has been used extensively as a complementary facility in several machines, for example: UNU/ICTP PFF [3, 5, 7–9], NX2 [9, 11], NX1 [9], DENA [12]. It has also been used in other machines for design and interpretation including sub-kJ PF machines [13], FNII [14] and the UBA hard X-ray source [15]. Information computed includes axial and radial dynamics [3, 7, 16], SXR emission characteristics and yield [8, 9, 11, 17–22], design of machines [3, 5, 7–9, 17, 22, 23], optimization of machines [3, 7–9, 17] and adaptation to Filippov-type DENA [12]. Speed-enhanced PF [7] was facilitated. Plasma focus neutron yield calculations [24–26], current and neutron yield limitations [27, 28], deterioration of neutron scaling (neutron saturation) [29, 30], radiative collapse [31], current-stepped PF [32] and extraction of diagnostic data [33–35] and anomalous resistance data [36, 37] from current signals have been studied using the code [1]. The Model code has recently been used to produce reference numbers for deuteron beam number and energy fluence and flux and scaling trends for these with PF storage energy [38]. These beam properties were extended to all gases [39]. In the present paper we use the code to look at the neutron yield of PF1000 as a function of operating pressures.

Procedures for the Numerical Experiments

The Lee model code is configured to work as any plasma focus by inputting the bank parameters, inductance L_0, capacitance C_0 and stray circuit resistance r_0; the tube

S. H. Saw · S. Lee
INTI International University College, 71800 Nilai, Malaysia

S. H. Saw · S. Lee
Institute for Plasma Focus Studies, 32 Oakpark Drive, Chadstone, VIC 3148, Australia

D. Subedi · R. Shrestha · S. Dugu
Department of Natural Science, Kathmandu University, Dhulikhel, Nepal

R. Khanal (✉)
Central Department of Physics, Tribhuvan University, Kirtipur, Kathmandu, Nepal
e-mail: plasmanepal@hotmail.com

S. Lee
Universty of Malaya, Kuala Lumpur, Malaysia

Published online: 25 June 2014

Author's personal copy

parameters outer electrode (cathode) radius b, inner electrode (anode) radius a and anode length z_0; and operational parameters voltage V_0 and pressure P_0 and the fill gas. The standard practice is to fit the computed total discharge current waveform to an experimentally measured total discharge current waveform [1, 17, 19] using four model parameters representing the mass swept-up factor f_m, the plasma current factor f_c for the axial phase and factors f_{mr} and f_{cr} for the radial phases.

From experience it is known that the current trace of the focus is one of the best indicators of gross performance. The axial and radial phase dynamics and the crucial energy transfer into the focus pinch are among the important information that is quickly apparent from the current trace.

The exact time profile of the total current trace is governed by the bank parameters, by the focus tube geometry and the operational parameters. It also depends on the fraction of mass swept-up and the fraction of sheath current and the variation of these fractions through the axial and radial phases. These parameters determine the axial and radial dynamics, specifically the axial and radial speeds which in turn affect the profile and magnitudes of the discharge current. The detailed profile of the discharge current during the pinch phase also reflects the Joule heating and radiative yields. At the end of the pinch phase the total current profile also reflects the sudden transition of the current flow from a constricted pinch to a large column flow. Thus the discharge current powers all dynamic, electrodynamic, thermodynamic and radiation processes in the various phases of the plasma focus. This explains the importance attached to matching the computed current trace to the measured current trace in the procedure adopted by the Lee model code.

The Numerical Experiments-Fitting the Computed Current Trace to Obtain the Model Parameters

Gribkov et al. [40] had published a paper with laboratory measurements from the PF1000, including a typical current waveform and information on neutron yield at a typical pressure of 3.5 Torr. We first fit the computed current waveform to the published measured waveform.

We configure the Lee model code (version RADPF05.15) to operate as the PF1000 starting with the following published bank and tube parameters obtained from their paper:

Bank parameters:	$L_0 = 20$ nH (nominal), $C_0 = 1{,}332$ μF, r_0 = not given
Tube parameters:	b = 16 cm, a = 11.55 cm, $z_0 = 60$ cm
Operating parameters:	$V_0 = 27$ kV, $P_0 = 3.5$ Torr Deuterium

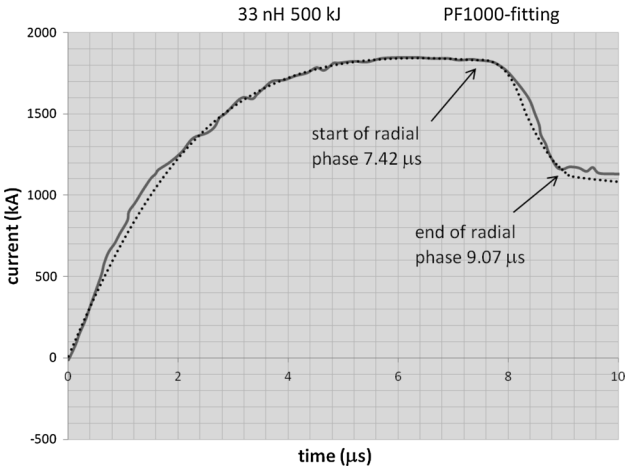

Fig. 1 Computed discharge current (*doted plot*) compared to published current for PF1000

To obtain a reasonably good fit the following bank and tube parameters (L_0 and r_0 fitted) are used:

Bank parameters:	$L_0 = 33$ nH, $C_0 = 1{,}332$ μF, $r_0 = 6.3$ mΩ
Tube parameters:	b = 16 cm, a = 11.55 cm, $z_0 = 60$ cm
Operating parameters:	$V_0 = 27$ kV, $P_0 = 3.5$ Torr Deuterium
Together with the following fitted model parameters:	$f_m = 0.13$, $f_c = 0.7$, $f_{mr} = 0.35$ and $f_{cr} = 0.65$

The fitted computed current waveform is compared with published waveform in Fig. 1.

The Numerical Experiments-Computing the Neutron Yield as a Function of Operating Pressure

Using the fitted inductance, stray resistance and model parameters, numerical experiments are then carried out at various initial pressures in Deuterium. The current waveforms obtained from these numerical experiments at various pressures are displayed in Fig. 2.

We discuss the change of current waveforms from very high pressures to low pressures. At very high pressures (a hypothetical 100,000 Torr at which pressure because of the extreme mass loading there is no plasma motion-equivalent to short-circuiting the plasma focus at its input end) the waveform is a damped sinusoid. Lowering the operational pressure, at 19 Torr the characteristic flattening of the current waveform due to dynamics is already clearly evident. The current peak comes earlier and is lower than the dynamically unloaded (high pressure) case, the current then droops until the rollover into the dip (due to the increased

Author's personal copy

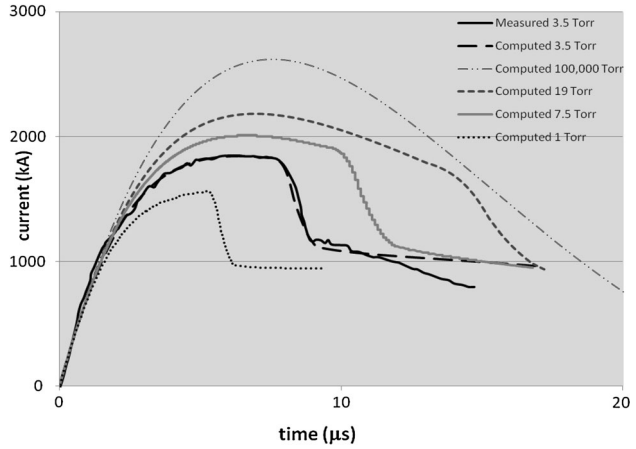

Fig. 2 Computed current waveforms as function of pressure. The basis of reference is a measured waveform at 3.5 Torr which is used to fit the computed 3.5 Torr waveform to obtain the model parameters. The fitted traces at 3.5 Torr are shown in this figure

radial phase loading) at around 15 μs. At still lower pressures these characteristics remain the same except that the current trace is depressed more and more as speed increases. The peaking (reaching maximum current) also comes earlier and earlier, as does the radial phase rollover (into the current dip) of the current trace. This is characteristic of an RLC circuit with increasing resistance R, as R increases from light towards critical damping. In the case of the plasma focus the increasing resistance is due to the dynamic resistance of the current sheet motion with increasing speed.

At 2.0 Torr, there is hardly any droop for the current trace, the current waveform showing a distinct flat top leading to the rollover. At 1 Torr the axial speed is now so high that the axial phase is completed in <5 μs and the current is still rising when it is forced down by the radial phase dynamics.

Plasma Focus Parameters as Functions of Pressures

The Lee model code is used to compute the neutron yield versus pressure curve of the Polish PF1000 facility [40], which has the largest bank operating on the energy level of about 1 MJ, and it operates with deuterium as a working gas. Some relevant properties of the PF1000 are computed and recorded in the following Table 1. To present these plasma focus properties on one chart for correlation purposes each property is normalized to its value at 7.5 Torr. We then obtain the following Table 2. Some of these properties are plotted in the following figures.

From the tables and Fig. 3 we see the following important salient features. Starting at high pressures e.g. 19 Torr, as P_0 decreases, I_{peak} decreases, and continues to decrease,

Table 1 Plasma focus properties of PF1000 for different pressure

P_0 (Torr)	I_{peak} (kA)	I_{pinch} (kA)	Axial peak v_a (cm μs^{-1})	Speed factor (S)	Radial peak v_s (cm μs^{-1})	Radial peak v_p (cm μs^{-1})	a_{min} (cm)	z_{max} (cm)	Pinch duration (ns)	Peak V (kV)	Tpinch max (10^6 K)	**Yn (10^10) n**	Nipinch max (10^{23} cm^{-3})	EINP (%)
100 k	2,610													
19	2,171	702	5.4	43	6.3	4.6	2.5	18.5	739	11.1	0.17	3.11	16.6	12.70
14	2,120	788	6	49	8.2	6.1	2.42	18.7	558.3	16.7	0.23	10	13.1	13.8
10	2,060	843	7	56	10.2	7.6	2.32	18.7	440.8	23.2	0.37	15	10.2	14.4
9	2,039	854	7.4	59	10.9	8.1	2.3	18.7	412.6	25.2	0.42	16	9.4	14.4
8	2,017	863	7.8	62	11.6	8.7	2.29	18.7	385.1	27.4	0.49	17	8.4	14.4
7.5	**2,004**	**867**	**8.3**	**63**	**11.5**	**8.5**	**2.24**	**18.7**	**371.2**	**27.7**	**0.49**	**17**	**8.2**	**14.41**
7	1,990	870	8.2	65	12.5	9.4	2.27	18.8	357.3	9.4	0.57	17	7.5	14.4
6	1,960	874	8.8	69	13.5	10.2	2.26	18.8	329.4	32.7	0.67	16	6.5	14.2
3.5	1,846	862	10.8	85	17.3	13.2	2.23	18.8	255	42.1	1.11	11.57	3.9	13.10
2	1,709	777	13.5	105	20.3	15.2	2.18	18.8	213.7	47	1.58	6	2.3	10.6
1	1,547	709	17	134	26.1	19.7	2.17	18.8	165.7	55.6	2.63	3	1.2	8.6

Bold numbers represent the values at 7.5 Torr

S = Speed factor [23] in kA cm^{-1} Torr$^{-1/2}$

Author's personal copy

Table 2 Plasma focus properties of PF1000 for different pressure (values normalised to value at 7.5 Torr)

P_0	I_{peak}	I_{pinch}	Axial peak v_a	Speed factor	Radial peak v_s	Radial peak v_p	a_{min}	z_{max}	Pinch duration	Peak V	Tpinch max	**Yn**	Nipinch max	EINP
All normalised to value at 7.5 Torr														
100 k	1.30													
19	1.08	0.81	0.65	0.68	0.55	0.54	1.12	0.99	1.99	0.40	0.35	0.18	2.02	0.88
14	1.06	0.91	0.72	0.78	0.71	0.72	1.08	1	1.50	0.60	0.47	0.59	1.60	0.96
10	1.03	0.97	0.84	0.89	0.89	0.89	1.04	1	1.19	0.84	0.76	0.88	1.24	1
9	1.02	0.98	0.89	0.94	0.95	0.95	1.03	1	1.11	0.91	0.86	0.94	1.15	1
8	1.01	0.99	0.94	0.98	1.01	1.02	1.02	1	1.04	0.99	1	1	1.02	1
7.5	**1**	**1**	**1**	**1**	**1**	**1**	**1**	**1**	**1**	**1**	**1**	**1**	**1**	**1**
7	0.99	1.00	0.99	1.03	1.09	1.11	1.01	1.01	0.96	0.34	1.16	1	0.91	1
6	0.98	1.01	1.06	1.10	1.17	1.20	1.01	1.01	0.89	1.18	1.37	0.94	0.79	0.99
3.5	0.92	0.99	1.30	1.35	1.50	1.55	0.99	1.01	0.69	1.52	2.27	0.68	0.48	0.91
2	0.86	0.95	1.59	1.67	1.89	1.95	0.99	1.01	0.55	1.84	3.10	0.41	0.27	0.80
1	0.78	0.82	2.06	2.14	2.29	2.33	0.97	1.01	0.44	2.05	5.47	0.18	0.15	0.65

Bold numbers represent the values at 7.5 Torr

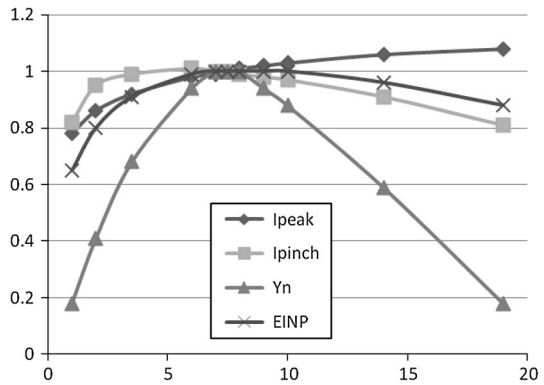

Fig. 3 Selected PF1000 normalized properties (Y_n, I_{peak}, I_{pinch} and EINP) versus pressure. *Horizontal axis* represents pressure in Torr; *vertical axis* values are in normalised units

because the increasing axial speed increases the circuit loading, throughout the whole range of pressures. However it is noticed that I_{pinch} increases from high pressures, peaking in a flat manner at 6 Torr and then decreases sharply as pressure is reduced towards 1 Torr. One factor contributing to the increase is the shift of the pinch time from very late in the discharge (when discharge current has dropped greatly) to earlier in the discharge (when current has dropped less). That is the main factor for I_{pinch} increasing despite a decreasing I_{peak}. At low pressures (e.g. 1 Torr), the radial phase now occurs so early that it is forcing the current down early in the discharge. That lowers both the I_{peak} as well as the I_{pinch}. These points are clear when you look at the comparative chart of current traces at various pressures.

The radial EINP follows the same pattern as I_{pinch}, and for the same reasons. The radial EINP computes the cumulative work done by the current sheath (piston) in the radial phases.

Looking at the other quantities, we note that the speeds (axial, radial shock and radial piston) and temperature all continue to rise as pressure lowers; similarly S and maximum induced voltage V also increase as pressure is decreased. Pinch length z_{max} is almost a constant. Minimum pinch radius and pinch duration continue to decrease; the former due to better compression at higher speeds and the latter due to the increased T. The number density progressively drops, due to the decreasing starting numbers, despite the increasing compression.

From the tabulations of the above numerical experiments, it might be useful to consider the beam-target mechanism which we are using to compute the neutron yield [24, 29].

$$Y_{b-t} = C_n n_i I_{pinch}^2 z_p^2 \left(\ln\left(b/r_p\right)\right)\sigma/V_{max}^{1/2}$$

where σ is the D–D fusion cross section. In the range we are considering we may take $\sigma \sim V_{max}^n$ where n ~ 2–3; say we take n = 2.5; then we have

$$Y_{b-t} \sim n_i I_{pinch}^2 z_p^2 \left(\ln\left(b/r_p\right)\right) V_{max}^2$$

From Table 1 we note that the factor $z_p^2(\ln(b/r_p))$ is practically constant.

Thus we note that it is the interplay of the behaviour of n_i, I_{pinch} and V_{max} as pressure changes that determines the way Y_n increases to a maximum and then drops as pressure is changed.

In their paper Gribkov et al. [40] have recorded that their Y_n at 3.5 Torr ranges from 3 to 7 $\times$ 10^{10} with maximum values of 2 $\times$ 10^{11} neutrons per shot. Our computed value of Y_n at 3.5 Torr is 9 $\times$ 10^{10}. This is comparable with their measured range of values.

Author's personal copy

Conclusion

We have used the Lee model code to run numerical experiments on the PF1000. The results of the code are linked to the real experiments through a measured current trace at 3.5 Torr. The computed neutron yield at this pressure point is found to be comparable to the published measured results. The computed neutron yield curve is then obtained to find the optimum neutron yield as a function of operating pressure. Correlation of the behavior of neutron yield with pressure is discussed in terms of the variation with pressure of plasma ion density n_i, I_{pinch} and induced voltage V_{max}.

Acknowledgments Two of the authors, S. L. and S. H. S. acknowledge research Grants INT-CPR-01-02-2012 and FRGS/2/2013/SG02/INTI/01/1 in the preparation of this paper during a collaborative research activity associated with the Asian African Association for Plasma Training (AAAPT).

References

1. S. Lee, Radiative dense plasma focus computation package: RADPF. http://www.plasmafocus.net; http://www.intimal.edu.my/school/fas/UFLF/ (archival websites) (2013)
2. S. Lee, in *Radiation in Plasmas* Vol II, ed. by B. McNamara, Process of Spring College in Plasma Physics (1983) ICTP, Trieste, pp. 978–987, ISBN 9971-966-37-9, Published: World Scientific Pub Co, Singapore (1984)
3. S. Lee, T.Y. Tou, S.P. Moo, M.A. Elissa, A.V. Gholap, K.H. Kwek, S. Mulyodrono, A.J. Smith, S. Suryadi, W. Usala, M. Zakaullah, Am. J. Phys. **56**, 62 (1988)
4. T.Y. Tou, S. Lee, K.H. Kwek, IEEE Trans. Plasma Sci. **17**, 311–315 (1989)
5. S.P. Moo, C.K. Chakrabarty, S. Lee, IEEE Trans. Plasma Sci. **19**, 515–519 (1991)
6. S. Lee, J. Fusion Energ. (2014). doi:10.1007/s10894-014-9683-8
7. A. Serban, S. Lee, Plasma Sour. Sci. Technol. **6**, 78 (1997)
8. M.H. Liu, X.P. Feng, S.V. Springham, S. Lee, IEEE Trans. Plasma Sci. **26**, 135 (1998)
9. S. Lee, P. Lee, G. Zhang, X. Feng, V.A. Gribkov, M. Liu, A. Serban, T. Wong, IEEE Trans. Plasma Sci. **26**, 1119 (1998)
10. S. Lee. http://ckplee.home.nie.edu.sg/plasmaphysics/ (archival website) (2013)
11. D. Wong, P. Lee, T. Zhang, A. Patran, T.L. Tan, R.S. Rawat, S. Lee, Plasma Sour. Sci. Technol. **16**, 116 (2007)
12. V. Siahpoush, M.A. Tafreshi, S. Sobhanian, S. Khorram, Plasma Phys. Control. Fusion **47**, 1065 (2005)
13. L. Soto, P. Silva, J. Moreno, G. Silvester, M. Zambra, C. Pavez, L. Altamirano, H. Bruzzone, M. Barbaglia, Y. Sidelnikov, W. Kies, Braz. J. Phys. **34**, 1814 (2004)
14. H. Acuna, F. Castillo, J. Herrera, A. Postal, International Conference on Plasma Science, 3–5 June 1996, Conference Record, p. 127
15. C. Moreno, V. Raspa, L. Sigaut, R. Vieytes, Appl. Phys. Lett. **89**, 091502 (2006)
16. S.H. Saw, M. Akel, P.C.K. Lee, S.T. Ong, S.N. Mohamad, F.D. Ismail, N.D. Nawi, K. Devi, R.M. Sabri, A.H. Baijan, J. Ali, S. Lee, J. Fusion Energ. **31**, 411 (2012)
17. S.H. Saw, P.C.K. Lee, R.S. Rawat, S. Lee, IEEE Trans. Plasma Sci. **37**, 1276 (2009)
18. S. Lee, R.S. Rawat, P. Lee, S.H. Saw, J. Appl. Phys. **106**, 023309 (2009)
19. S.H. Saw, S. Lee, Energ. Power Eng. **2**(1), 65 (2010)
20. M. Akel, S. Al-Hawat, S.H. Saw, S. Lee, J. Fusion Energ. **29**(3), 223 (2010)
21. M. Akel, S. Lee, S.H. Saw, IEEE Trans. Plasma Sci. **40**, 3290 (2012)
22. S. Lee, S.H. Saw, R.S. Rawat, P. Lee, A. Talebitaher, A.E. Abdou, P.L. Chong, F. Roy, A. Singh, D. Wong, K. Devi, IEEE Trans. Plasma Sci. **39**, 3196 (2011)
23. S. Lee, A. Serban, IEEE Trans. Plasma Sci. **24**, 1101 (1996)
24. S. Lee, S.H. Saw, J. Fusion Energ. **27**, 292 (2008)
25. S. Lee, S.H. Saw, L. Soto, S.V. Springham, S.P. Moo, Plasma Phys. Control. Fusion **51**, 075006 (2009)
26. S. Lee, S.H. Saw, L. Soto, S.V. Springham, S.P. Moo, Plasma Phys. Control. Fusion **51**, 075006 (2009)
27. S. Lee, S.H. Saw, Appl. Phys. Lett. **92**, 021503 (2008)
28. S. Lee, P. Lee, S.H. Saw, R.S. Rawat, Plasma Phys. Control. Fusion **50**, 065012 (2008)
29. S. Lee, Plasma Phys. Control. Fusion **50**, 10500 (2008)
30. S. Lee, Appl. Phys. Lett. **95**, 151503 (2009)
31. S. Lee, S.H. Saw, J. Ali, J. Fusion Energ. **32**, 42 (2013)
32. S. Lee, S.H. Saw, J. Fusion Energ. **31**, 603 (2012)
33. S. Lee, S.H. Saw, P.C.K. Lee, R.S. Rawat, H. Schmidt, Appl. Phys. Lett. **92**, 111501 (2008)
34. S.H. Saw, S. Lee, F. Roy, P.L. Chong, V. Vengadeswaran, A.S.M. Sidik, Y.W. Leong, A. Singh, Rev. Sci. Instrum. **81**, 053505 (2010)
35. S. Lee, S.H. Saw, R.S. Rawat, P. Lee, R. Verma, A. Talebitaher, S.M. Hassan, A.E. Abdou, M. Ismail, A. Mohamed, H. Torreblanca, S. Al-Hawat, M. Akel, P.L. Chong, F. Roy, A. Singh, D. Wong, K.K. Devi, J. Fusion Energ. **31**, 198 (2012)
36. R.A. Behbahani, F.M. Aghamir, J. Appl. Phys. **111**(4), 043304 (2012)
37. R.A. Behbahani, F.M. Aghamir, Phys. Plasmas **18**, 103302 (2011)
38. S. Lee, S.H. Saw, Phys. Plasmas **19**, 112703 (2012)
39. S. Lee, S.H. Saw, Phys. Plasmas **20**, 062702 (2013)
40. V.A. Gribkov, A. Banaszak, B. Bienkowska, A.V. Dubrovsky, I. Ivanova-Stanik, L. Jakubowski, L. Karpinski, R.A. Miklaszewski, M. Paduch, M.J. Sadowski, M. Scholz, A. Szydlowski, K. Tomaszewski, J. Phys. D Appl. Phys. **40**, 3592 (2007)